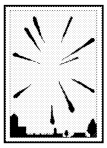

Meteoritics & Planetary Science 38, Nr 8, 1187–1197 (2003)
Abstract available online at http://meteoritics.org

Scanning electron microscopy, cathodoluminescence, and Raman spectroscopy of experimentally shock-metamorphosed quartzite

Arnold GUCSIK,[1] Christian KOEBERL,[1*] Franz BRANDSTÄTTER,[2]
Eugen LIBOWITZKY,[3] and Wolf Uwe REIMOLD[4]

[1]Department of Geological Sciences, University of Vienna, Althanstrasse 14, A-1090 Vienna, Austria
[2]Department of Mineralogy, Natural History Museum, P.O. Box 417, A-1014 Vienna, Austria
[3]Institute of Mineralogy and Crystallography, University of Vienna, Althanstrasse 14, A-1090 Vienna, Austria
[4]Impact Cratering Research Group, School of Geosciences, University of Witwatersrand, Private Bag 3, P.O. 2050, Johannesburg, South Africa
[*]Corresponding author. E-mail: christian.koeberl@univie.ac.at

(Received 30 December 2002; revision accepted 8 July 2003)

Abstract–We studied unshocked and experimentally (at 12, 25, and 28 GPa, with 25, 100, 450, and 750°C pre-shock temperatures) shock-metamorphosed Hospital Hill quartzite from South Africa using cathodoluminescence (CL) images and spectroscopy and Raman spectroscopy to document systematic pressure or temperature-related effects that could be used in shock barometry. In general, CL images of all samples show CL-bright luminescent patchy areas and bands in otherwise non-luminescent quartz, as well as CL-dark irregular fractures. Fluid inclusions appear dominant in CL images of the 25 GPa sample shocked at 750°C and of the 28 GPa sample shocked at 450°C. Only the optical image of our 28 GPa sample shocked at 25°C exhibits distinct planar deformation features (PDFs). Cathodoluminescence spectra of unshocked and experimentally shocked samples show broad bands in the near-ultraviolet range and the visible light range at all shock stages, indicating the presence of defect centers on, e.g., SiO_4 groups. No systematic change in the appearance of the CL images was obvious, but the CL spectra do show changes between the shock stages. The Raman spectra are characteristic for quartz in the unshocked and 12 GPa samples. In the 25 and 28 GPa samples, broad bands indicate the presence of glassy SiO_2, while high-pressure polymorphs are not detected. Apparently, some of the CL and Raman spectral properties can be used in shock barometry.

INTRODUCTION

Cathodoluminescence (CL) is an optical phenomenon that is based on the generation of visible radiation through sample excitation by high-energy electrons (in general, with energies of the incident beam of 5–25 kV, the depth of penetration is 1–3 μm). Wavelengths of the cathodoluminescence emissions range from the ultraviolet (UV) to the infrared (IR) and result from a variety of defects (e.g., various structural imperfections such as poor ordering, radiation damage, and shock damage) and impurities in the crystal structure of a mineral (Marshall 1988; Hayward 1998).

Luminescence can have 2 causes: intrinsic CL, which is characteristic of the host material, and extrinsic CL, which results from impurities. 1) Intrinsic luminescence is enhanced by vacancies, poor ordering, radiation damage, and shock damage as structural imperfections and impurities (non-activators), which distort the crystal lattice (Marshall 1988). 2) Extrinsic luminescence is caused by impurities or activator elements, which are also referred to as sensitizers. Their presence is necessary to create a luminescence center with an activator mineral (Marshall 1988; Hayward 1998). It is important to note that quenchers, such as Fe^{3+}, Fe^{2+}, and Co^{2+}, show broad and intense charge transfer bands in the absorption spectrum and cause quenching of the luminescence of activators with interfering emission bands (Marshall 1988; Hayward 1998).

So far, no systematic study has been made regarding the changes of CL properties (optical appearance in CL images and the characteristics of CL spectra) with shock pressure in quartz, although CL petrography of impact-related carbonates has been described (Fouke et al. 2002). As quartz is one of the most common rock-forming minerals, for which ample information on shock-related changes of a large variety of mineralogical, crystallographic, and petrographic parameters exists (e.g., Stöffler and Langenhorst 1994; Langenhorst and

Deutsch 1994; Grieve et al. 1996; Huffman and Reimold 1996), we undertook such an investigation.

The CL luminescence emission in the unshocked quartz might be associated with defect structures. The silicon dioxide structure is modified by different types of defect structures (impurities, vacancies, etc.), which occur in the short range order. Hence, similar types of defects are found in crystalline and amorphous polymorphs of silicon dioxide (Stevens Kalceff et al. 2000, and references therein). Generally, the luminescence of quartz shows different CL colors depending on its origin. CL studies have been performed on fractured quartz (e.g., Milliken and Laubach 2000, and references therein) and for provenance studies (e.g., Ramseyer and Mullis 2000; Götze et al. 2001, and references therein). Serebrennikov et al. (1982) studied thermoluminescence properties of shocked quartz, but previous work on CL properties of shocked quartz is limited. Owen and Anders (1988), in a pioneering study, showed that quartz from intrusive igneous and high-grade metamorphic rock shows darker purple-blue CL, while quartz from low-grade metamorphic rocks exhibits reddish-brown CL, and that shocked quartz from the Cretaceous-Tertiary (K/T) boundary exhibits CL colors similar to those of low-grade metamorphic quartz. Owen and Anders (1988) used these observations to demonstrate that shocked quartz from the K/T boundary was not derived from volcanic sources. At that time (1988), this was an important contribution to the study of the then controversial origin of the K/T boundary. Ramseyer et al. (1992) reported CL luminescence changes for quartz and feldspar from the granitic rocks of the Siljan impact structure, Sweden, and related their findings to complex alteration of the minerals during a post-impact hydrothermal overprint. Seyedolali et al. (1997) reported CL studies of shocked quartz grains from the Mjølnir impact structure (Barents Sea) in comparison with quartz from a variety of other sources. These authors studied patterns of variable-intensity CL, including zoning, healed fractures, complex fractures, complex shears, and planar microdeformations from different source rocks using a combined scanning electron microscopy (SEM)-CL fabric-analysis technique. Ramseyer and Mullis (2000) briefly noted that quartz affected by meteorite impact or lightning is characterized by red CL of about 630 nm, but they do not give any detailed information.

More recently, Boggs et al. (2001) studied planar deformation features (PDFs) in shocked quartz from the Ries crater, Germany, using a SEM-CL imaging facility. They found that (in contrast to planar microstructures associated with tectonic fracturing) these features are filled by amorphous silica and appear as dark lines in the CL images, which indicates the absence of recombination centers for the emission of photons.

Micro-Raman spectroscopy is a technique that provides information on molecular vibrations (lattice vibrations in a crystal) from relatively small sample volumes (comparable to that analyzed by an electron microprobe). The resulting spectral bands depend upon the crystal structure (with its symmetry), the vibrating atoms (with their masses), and the forces between them. Well-crystallized quartz shows a number of vibrational bands between 128 and 1163 cm^{-1} that are localized in specific regions (Etchepare et al. 1974), i.e., >1050 and 700–800 cm^{-1} (Si-O stretching modes), 350–500 cm^{-1} (O-Si-O bending modes), and <300 cm^{-1} (Si-O-Si bending and torsional/twisting modes). Note that the Raman spectra of quartz are dominated by only one intense band at ~464 cm^{-1} (beside weaker bands), whereas IR spectra show intense bands both in the stretching and O-Si-O bending regions.

The study of Raman properties of unshocked and experimentally shock-deformed minerals (e.g., quartz) has the potential to provide a tool that can be used in shock barometry and to supplement the methods available so far, i.e., optical microscopy, X-ray, and density measurements (cf., Stöffler and Langenhorst 1994). Micro-Raman spectroscopy is, by now, a fairly routine technique that is not too complicated in its use (unlike the Nuclear Magnetic Resonance [NMR] technique; see, e.g., Cygan et al. 1990). Identification of a Raman spectroscopic method that would allow one to: a) identify shocked minerals, and b) give information on the shock pressure would be useful for the identification and study of impact structures.

However, only a few Raman studies on shock metamorphosed minerals from impact environments have been carried out so far. McMillan et al. (1992) were the first to study shocked quartz with Raman bulk methods. Champagnon et al. (1996) investigated quartz that was experimentally shocked in the range of 22 to 32 GPa by micro-Raman spectroscopy. However, some studies of glasses and of high-pressure polymorphs of quartz exist (cf., Boyer et al. 1985) that are relevant to impact studies. These include the investigation of the Raman properties of coesite from the Vredefort dome, South Africa (Halvorson and McHone 1992), coesite in suevite from the Chicxulub impact structure, Mexico (Lounejeva et al. 2002; Ostroumov et al. 2002), natural and synthetic coesite (Boyer et al. 1985), the coesite-stishovite transition (e.g., Serghiou et al. 1995), the densification behavior of silica glasses in shock experiments (Okuno et al. 1999), and tektites and impact glasses (Faulques et al. 2001)

The pre-shock temperature of the target rock also influences the formation and crystallographic orientation of PDFs. Reimold (1988), Huffman et al. (1993), and Huffman and Reimold (1996) presented the results of shock experiments with quartzite and granite at room temperature (25°C) and preheated to 450°C and 750°C. They noticed a distinct difference in the relative abundances of the $\{10\bar{1}3\}$ and $\{10\bar{1}2\}$ orientations and a large difference in the number of sets of PDFs per grain. Langenhorst et al. (1992) and Langenhorst and Deutsch (1994) used oriented single crystal

quartz samples at pressures of 20 to 40 GPa and temperatures of 20, 275, 540 and 630°C. They observed that development of PDFs and their orientation is a function of peak pressure, pre-shock temperature, and orientation of the crystal structure relative to the propagation direction of the shock wave.

Here, we present the results of cathodoluminescence (CL) and Raman spectroscopic observations obtained on experimentally shocked and partly preheated quartzite samples (Hospital Hill quartzite, Witwatersrand, South Africa). The purpose of this investigation is to explore the capability of the SEM-CL/micro-Raman technique to document shock effects and to determine whether CL effects in quartz are characteristic for particular shock pressure stages.

SAMPLES AND EXPERIMENTAL PROCEDURES

A sample from the Hospital Hill quartzite formation (Lower Witwatersrand Supergroup = West Rand Group) was obtained from a locality about 20 km west of Johannesburg (Reimold and Hörz 1986). This particular rock type was chosen because it occurs, naturally shock deformed, in the central uplift of the Vredefort impact structure, the Vredefort dome. The samples used in this study and previously described by Reimold and Hörz (1986), Huffman et al. (1993), and Huffman and Reimold (1996) show virtually no accessory phases (sericite <1 vol%); evidence of tectonic deformation was restricted to occasional weak subgrain development and rare tectonic lamellae. The samples were cut into plates of about 1 mm thickness and embedded in density-matching epoxy material. Shock recovery experiments were performed using an explosive wave generator. For comparison with naturally shocked material, these specimen were subjected to experimental shock at pressures of 12, 25, and 28 GPa at room temperature (25°C) and preheated to 100, 450, and 750°C, respectively (for further details, see Huffman and Reimold [1996] and Huffman et al. [1993]). In these quartzite samples, the previous authors found shock-induced microstructures, such as extension cracks, brecciation, planar deformation features, mosaicism, partial isotropization, and diaplectic glass.

For our studies, we used polished thin sections of fresh chips (i.e., not the same thin sections) of the same material. The samples were first examined under a petrographic microscope, and optical images were captured digitally. The samples were then carbon-coated and examined with an Oxford Mono-CL system attached to a JEOL JSM 6400 scanning electron microscope (SEM) at the Department of Mineralogy, Natural History Museum, Vienna, Austria. The operating conditions for all SEM-CL investigations were 15 kV accelerating voltage and 1.2 nA beam current; backscattered-electron (BSE) and cathodoluminescence (CL) images were obtained from areas of approximately 450 × 450 µm. CL spectra were recorded in the wavelength range of 200–800 nm, with 1 nm resolution using a photo-multiplier detector. The acquisition time of each CL spectrum was 18 min, whereas CL images were obtained within scanning times of about 1 min. The grating of the monochromator was 1200 lines/mm. The CL spectra were obtained from approximately 40 × 40 µm areas.

The Raman spectra were obtained with a Renishaw RM1000 confocal micro-Raman spectrometer with a 20 mW, 632 nm He-Ne-laser excitation system and a thermo-electrically cooled CCD detector at the Institute of Mineralogy and Crystallography, University of Vienna, Vienna, Austria. The power of the laser beam on the sample was approximately 3 mW. The spectra were obtained in the range of 100–1200 cm^{-1}, with approximately a 30 sec acquisition time. The spectral resolution (apparatus function) was 4 cm^{-1} using a grating with 1200 grooves/mm. The Raman spectra were taken in confocal mode from a $3 \times 3 \times 3$ μm^3 sample volume using a Leica DMLM microscope and a Leica 50×/0.75 N.A. objective. Unfortunately, the quality of some of the Raman spectra is not ideal, and we have tried to reacquire the Raman spectra of the 25 and 28 GPa shocked quartzite samples. The samples had suffered irreversible changes in SEM/CL, i.e., the samples no longer display nice, glassy SiO_2 spectra but, rather, an incredibly large luminescence background, which does not allow us to identify any real spectral features.

Three CL spectra and three Raman spectra of different areas were acquired per sample, and, as no significant intrasample variations appeared to exist, only representative images and spectra are shown in the following figures.

RESULTS

According to Reimold and Hörz (1986) and Huffman et al. (1993), the experimentally shocked Hospital Hill quartzite specimens show the usual progression, with increasing shock intensity, from random fractures (at 5 GPa) to the development of planar fractures (16 GPa) and mosaic structure (at 25 GPa), to single sets of PDFs, to multiple sets of PDFs, and finally, to isotropization (at 30 GPa) and partial melting (35 GPa). Reimold (1988) noted that pervasive fracturing, brecciation, and shock mosaicism are better developed at comparatively lower shock pressures in the preheated specimens. As the development of mosaicism proceeds, random fracturing decreases in abundance and planar fractures appear. PDFs first appear at 16.8 GPa in the cold shocked sample but were not observed at 17.5 GPa in the preheated specimen (these samples were not available for the present study). This could reflect inhomogeneous pressure distribution in the disks during shock experiments.

Cathodoluminescence (CL) Image Observations

Unshocked Sample

Relatively CL-bright patchy areas and bands that are transected by irregular CL-dark fractures in non-luminescent quartzite are visible in the CL images (Fig. 1a). We did not

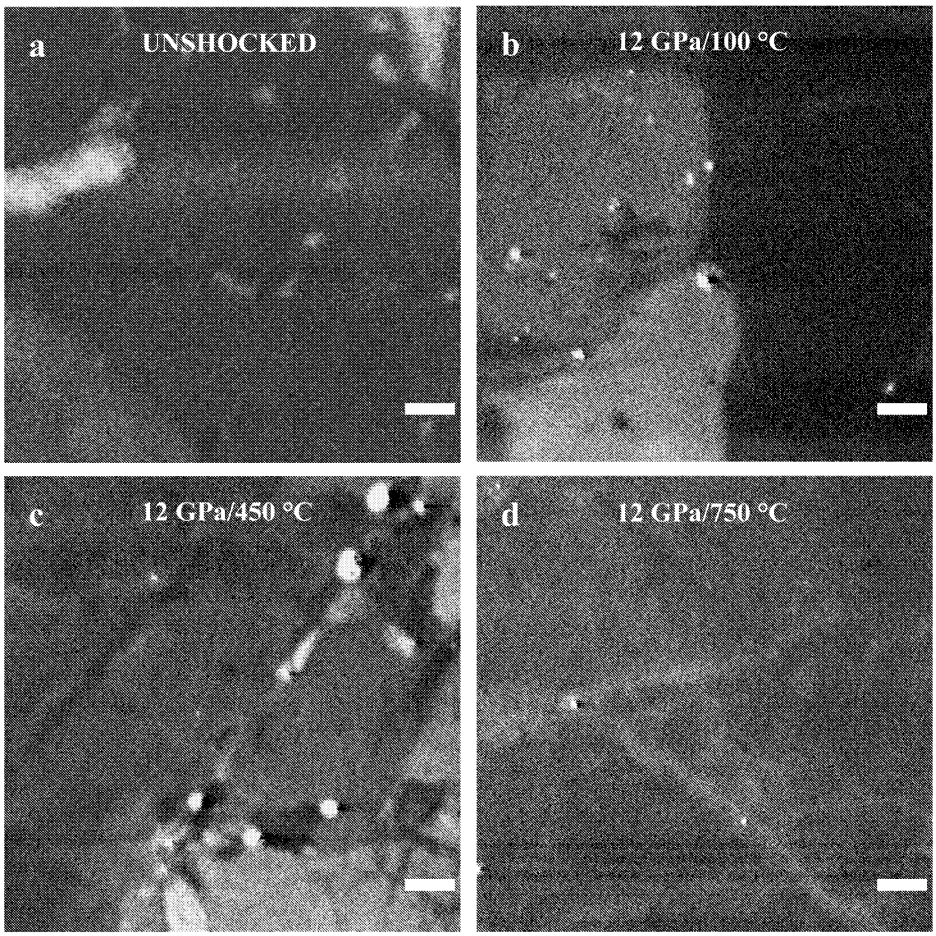

Fig. 1. Representative cathodoluminescence images of an unshocked quartzite from Hospital Hill, Witwatersrand Supergroup, and a quarzite (same location) shocked to 12 GPa. The images suffer somewhat from the very low luminosity of the quartz (i.e., bad signal to noise ratio). The white scale bar is 30 μm long: a) the CL-bright patchy areas and bands are transected by irregular CL-dark fractures in non-luminescent quartzite of the unshocked sample; b) the sample shocked at 12 GPa and 100°C shows rounded areas with variations in CL intensity in otherwise non-luminescent quartzite; c) the sample shocked to 12 GPa at 450°C exhibits light-colored lenses along the irregular fractures; d) no fractures are visible in the CL image of the sample shocked to 12 GPa at 750°C.

observe irregular or subparallel fractures in the BSE images as in the previous optical studies (e.g., Reimold and Hörz 1986). Fluid inclusions and zonation patterns are not evident in the CL images (Fig. 1a).

Samples Shocked to 12 GPa at 100, 450, and 750°C

Shock mosaic texture and other shock-induced microdeformations (e.g., planar fractures), as described by Huffman et al. (1993), were not observed in our BSE images of 12 GPa samples. The sample shocked at 100°C shows areas with variations in CL intensity in otherwise non-luminescent quartzite (Fig. 1b). The sample shocked at 450°C exhibits light lenses along irregular fractures, which have a strong contrast to the CL-bright (with variations in CL intensity) luminescent background (Fig. 1c). According to the optical microscopy observations, these CL-bright lenses might be related to the recrystallization of quartz, which occurred along fractures. No fractures are visible in the CL mode of the sample shocked at 750°C (Fig. 1d). The randomly distributed light spots could be impurities. Some CL-bright bands are noted in the otherwise non-luminescent quartz.

Sample Shocked to 25 GPa at 750°C

Numerous relatively small, somewhat rounded CL-dark areas are visible in the sample shocked at 25 GPa and 750°C in otherwise luminescent quartz (Fig. 2a). These dark spots might be associated with fluid inclusions, which were probably part of the somewhat heterogeneous natural quartzite. A straight fracture in the upper left corner of the CL image shows relatively stronger CL luminescence than the surrounding area, perhaps indicating an effect related to the recrystallization of quartz.

Samples Shocked to 28 GPa at 25, 450, and 750°C

TEM investigations of microstructures in the samples shocked at 28 GPa and 25°C exhibit a well-developed shock mosaic structure along very narrow (≤1 μm) PDFs parallel to the π plane (Huffman et al. 1993). These authors noted that

the multiple intersecting sets of PDFs are oriented parallel to the (r) and (c) planes.

The CL image of this sample shows a weakly luminescing background (Fig. 2b). Only few relatively CL-bright patchy areas are visible, which might be related to the inhomogeneous distribution of activator elements such as Al and Ti (Marshall 1988; Hayward 1998). Compared to the sample shocked to 25 GPa at 750°C, the 28 GPa/450°C sample contains more CL-dark circular areas with CL-bright rims (Fig. 2c). This could indicate the presence of fluid inclusions in this particular quartzite sample. The CL image of the sample shocked to 28 GPa at 750°C shows CL-bright patchy areas and bands in an otherwise weakly luminescent background, which might be associated with the distribution of activator elements (Fig. 2d).

The optical (transmitted light) image of our 28 GPa/25°C sample exhibits multiple sets of PDFs with the following characteristics (Fig. 3a). These <1 μm wide, parallel, straight microdeformations are spaced at 1 to 2 μm with 3 orientations. Interestingly, none of the optically visible PDFs appear in our BSE and CL images (Figs. 3b and 3c). Both optical and TEM data showed that a distinction exists between PDFs in experimentally and naturally shocked quartz-bearing materials. The former PDFs are usually less apparent, whereas the latter display quite well-observable lamellae, often decorated with bubbles.

Raman Spectroscopy

Unshocked Sample and Samples Shocked to 12 GPa at 100, 450, and 750°C

Raman spectra of the unshocked sample and of all 12 GPa samples (at 100, 450, and 750°C) do not show significant differences (Fig. 4). Besides several very weak bands, the samples exhibit pronounced peaks at 127, 206, 264, 354, and 464 cm^{-1} (very strong!), which are

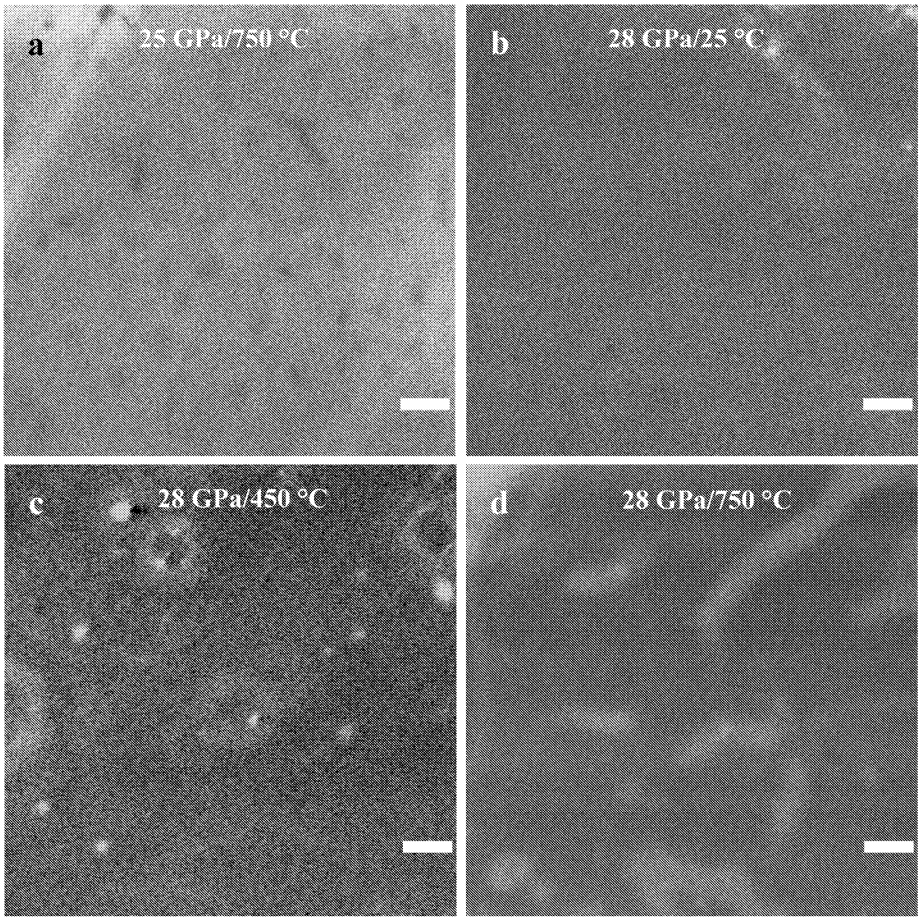

Fig. 2. Representative cathodoluminescence images of Hospital Hill quartzite samples shocked to 25 and 28 GPa. The white scale bar is 30 μm long: a) a high density of relatively small, CL-dark spots cluster to concentric features in the sample shocked at 25 GPa and 750°C within otherwise luminescent quartz, indicating the presence of fluid inclusions; b) the sample shocked at 28 GPa and 25°C exhibits a rather featureless and CL-dark image; c) the sample shocked at 28 GPa and 450°C contains well-developed CL-dark circular areas with CL-bright rims; d) the CL image of the sample shocked at 28 GPa and 750°C shows CL-bright patchy areas and bands set within an otherwise weakly luminescent background.

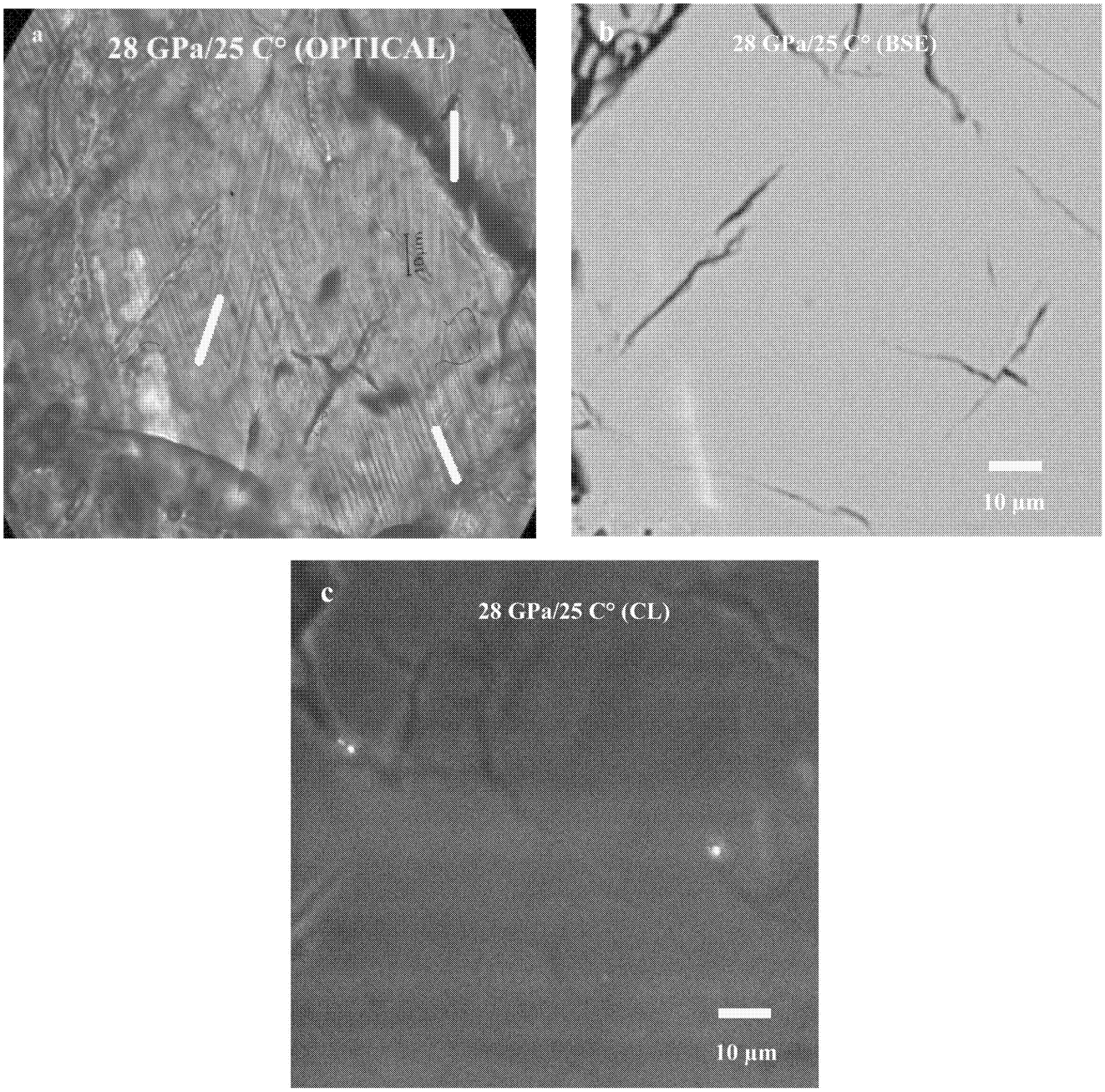

Fig. 3. Representative images of the same area with a Hospital Hill quartzite sample shocked at 28 GPa: a) optical (transmitted light); b) backscattered-electron image (BSE); and c) cathodoluminescence (CL) images of the 28 GPa/25°C sample of the Hospital Hill quartzite sample. The BSE image exhibits variations in BSE intensities and irregular fractures in these regions. The CL image shows CL-dark grain boundaries, which are transected by areas that are slightly less luminescent. Three discernable orientations (white bars) of well-developed, closely-spaced, parallel planar deformation features (PDFs) are observed. None of these features are visible in the BSE or CL images.

characteristic for quartz. Additionally, the background intensity is increased in the 12 GPa sample at 750°C (Fig. 4).

Samples Shocked to 25 GPa at 750°C and to 28 GPa at 25, 450, and 750°C

Except for a higher background intensity in the 28 GPa/25°C sample, the Raman spectra of the samples shocked to 25 GPa at 750°C and to 28 GPa (at 25, 450, and 750°C) are very similar but have a different appearance from the spectra of samples shocked at lower pressures and from the unshocked one. These samples do not show the dominant vibrational peak at 464 cm^{-1} but contain 2 broad bands centered at about 486 and 820 cm^{-1} (Fig. 5). These 2 broad bands indicate the transformation of quartz to diaplectic SiO_2 glass. Note that no other sharp bands exist that could indicate the presence of high-pressure SiO_2 polymorphs.

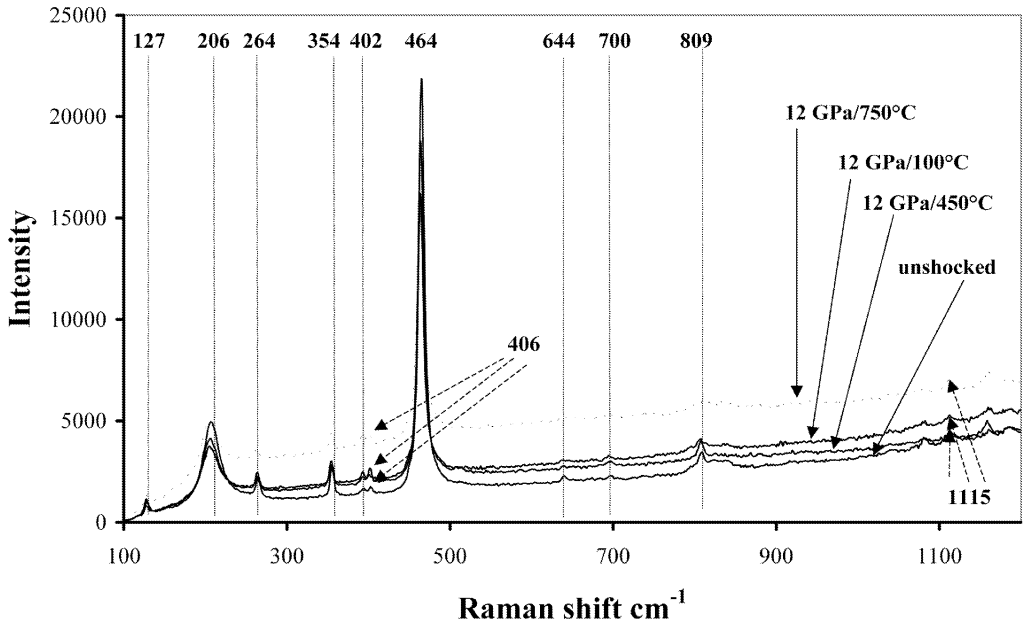

Fig. 4. Raman spectra of the unshocked and 12 GPa samples (at 100, 450, and 750°C) of the Hospital Hill quartzite do not show significant differences. The numbers denote peak positions in cm^{-1}.

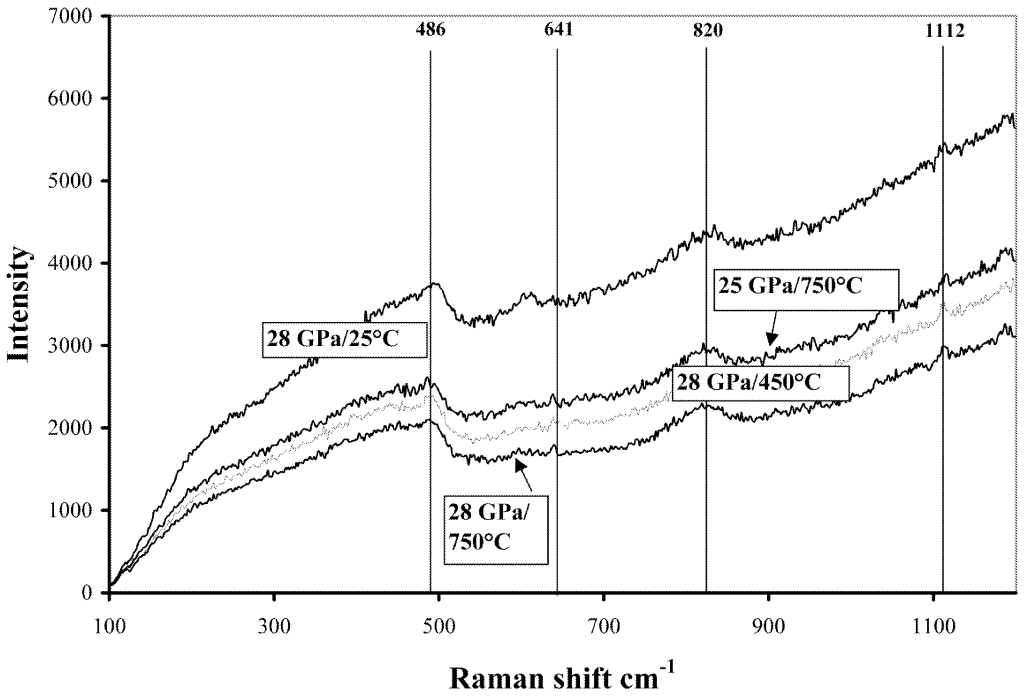

Fig. 5. Raman spectra of the 25 GPa (at 750°C) and 28 GPa (at 25, 450, and 750°C) samples of the Hospital Hill quartzite do not exhibit narrow peaks but 2 broad bands at about 486 and 820 cm^{-1}. The numbers denote approximate peak positions in cm^{-1}.

Cathodoluminescence Spectroscopy

We obtained cathodoluminescence spectra for quartzite and for the epoxy and glass onto which the quartzite specimens were mounted. This established that neither the epoxy nor the glass contribute to the broad bands observed in the CL spectra for these samples. To avoid duplication, we show only one of the typical spectra obtained for each sample.

Unshocked Sample

The CL spectrum of the unshocked sample (Fig. 6) exhibits 2 broad bands centered at 336 nm (3.68 eV) in the

near-ultraviolet range and at 616 nm (2.01 eV) in the visible light range. A sharp emission line appears at 696 nm (1.78 eV), showing a relatively high peak intensity (Fig. 6). This emission line is probably associated with Al impurities in the quartz and seems to be a short-time CL effect (cf., Perny et al. 1992), as it appeared in only one of our replicate spectra.

Samples Shocked to 12 GPa at 100, 450, and 750°C

The CL spectra of all shocked samples have an appearance that is significantly different from that of the unshocked sample. The CL spectrum of the sample shocked to 12 GPa at 100°C exhibits a significant broad band, which is centered at 426 nm (2.91 eV) in the visible light range. Additionally, a minor broad band is centered at 288 nm (4.3 eV) (Fig. 6). The 12 GPa sample shocked at 450°C shows a broad band centered at 372 nm (3.33 eV) in the near-ultraviolet range (Fig. 6). The 12 GPa sample shocked at 750°C exhibits a broad band, which is centered at 368 nm (3.36 eV) in the near-ultraviolet range (Fig. 6).

Samples Shocked to 25 GPa at 750°C and 28 GPa at 25, 450, and 750°C

The sample shocked to 25 GPa at 750°C shows a broad band in the near-ultraviolet range between about 300 and 400 nm, centered around 350 nm, with some minor peaks in the 384 nm (3.22 eV) region (Fig. 7).

The CL spectra of the 3 samples shocked at various temperatures to 28 GPa are similar to each other by showing a broad band with a maximum between about 440 and 460 nm (Fig. 7), which causes the blue luminescence of these samples. The CL spectrum of the sample shocked at 25°C has a broad band centered at 444 nm (2.79 eV), the broad peak or band in the one shocked at 450°C is centered at 454 nm (2.73 eV), and the one shocked at 750°C has the broad band centered at 462 nm (2.68 eV). The sample shocked at 450°C has the highest emission intensity in both band and background.

Differences Between CL Spectra

The spectra of the unshocked and shocked samples show significant differences in positions and intensities of broad peaks or bands. In general, the background intensity is relatively higher in the unshocked sample than in the samples experimentally shocked to 12 GPa. Compared to the unshocked sample, the shocked specimens do not contain narrow emission lines.

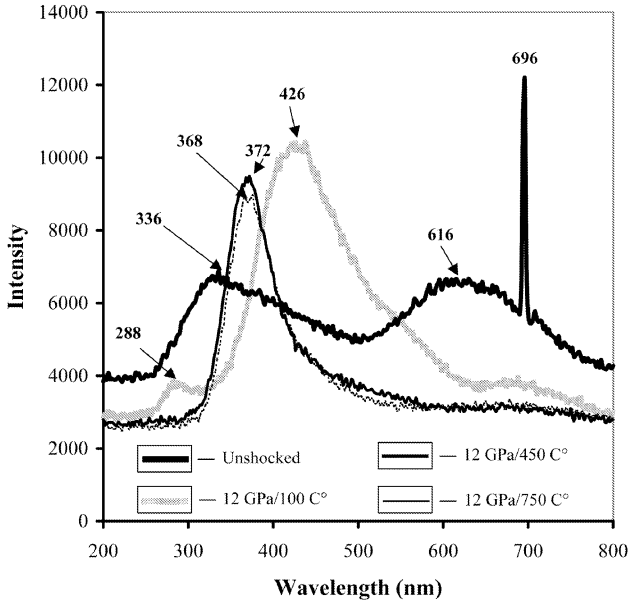

Fig. 6. Cathodoluminescence spectra of the unshocked Hospital Hill quartzite sample and 3 samples shocked to 12 GPa at 100, 450, and 750°C, respectively. The unshocked sample exhibits 2 broad bands that are centered at 336 nm in the near-ultraviolet range and at 616 nm in the visible light range. These broad bands might be related to defects in the deformed lattice, e.g., SiO_4^{4-}-groups. A narrow emission line appears at 696 nm, which indicates the presence of an activator; this line was seen in only one of our replicate spectra. The numbers denote peak positions in nm. In the shocked samples, a shift of the broad maximum toward higher wavelengths and a change in the shape and intensity of the Raman bands exist. The second broad band centered at ~616 nm disappears in the shocked samples.

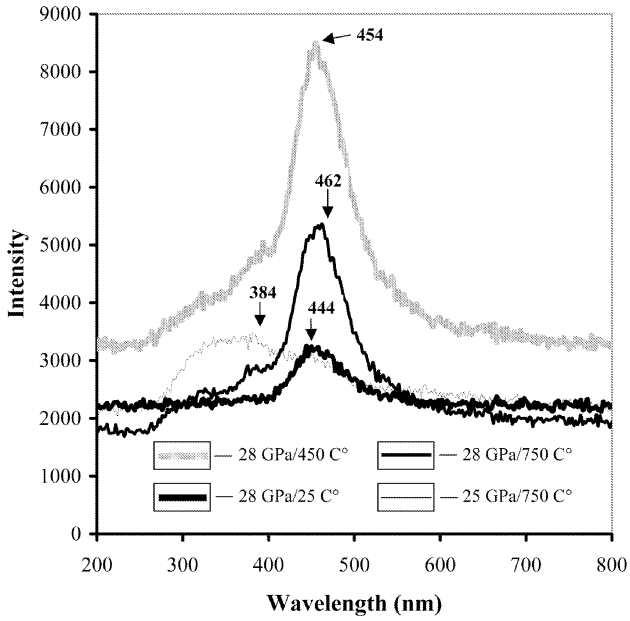

Fig. 7. Cathodoluminescence spectra of the Hospital Hill quartzite sample shocked to 25 GPa at 750°C and 3 samples shocked to 28 GPa at 25, 450, and 750°C, respectively. The 25 GPa sample at 750°C shows a broad band centered at 384 nm in the near-ultraviolet range. All 3 samples shocked at 28 GPa have broad peaks or bands within the 440 to 460 nm wavelength range, which causes blue luminescence of the samples. The CL spectrum of the sample shocked to 28 GPa at 25°C contains a broad band centred at 444 nm. The one shocked at 450°C has the band centered at 454 nm, whereas the sample shocked at 750°C has the band centered at 462 nm. This spectrum of the 28 GPa/450°C sample exhibits the highest band and background intensities. These broad bands are probably related to defects in the deformed lattice, e.g., SiO_4^{4-}-groups. The numbers denote peak positions in nm.

The unshocked sample has 2 broad bands centered around 336 and 616 nm, which are absent in the samples shocked at 12 GPa. These samples contain only 1 wide band, which is somewhat more narrow and has a relatively higher intensity than those of the unshocked sample. Figure 6 indicates that the broad band in the red part of the spectrum of the unshocked sample, at 616 nm, is still weakly visible in the sample shocked to 12 GPa at 100°C but is shifted further toward the red (around 700 nm). Moreover, this band disappears completely in the samples shocked at higher temperatures. In addition, the intensity of the band around 336 nm in the unshocked sample increases in the samples shocked to 12 GPa and is shifted toward higher wavelengths (~426 nm in the sample shocked at 100°C and about 370 nm in the samples shocked to 450 at 750°C). In the samples shocked to 25 and 28 GPa, the same broad band seems to be shifted even further from the ultraviolet region of the spectrum, up to ~460 nm (Fig. 7).

DISCUSSION

Raman Spectroscopy

Seifert et al. (1982) identified very strong (vs), strong (s), and medium (m) intensity Raman bands in vitreous SiO_2 at 440 (vs), 495 (vs), 605 (m), 810 (s), 1060 (m), and 1195 cm^{-1}. Raman spectra of quartz measured from 23 to 800°C for pressures between 0.1 MPa and 2.1 GPa have been described by Schmidt and Ziemann (2000). They found changes in frequency and line-width of the 206 and 464 cm^{-1} A_1 Raman modes. The positions and widths of peaks in the Raman spectra of our unshocked and 12 GPa samples are in good agreement with these previous studies. Raman spectra and characteristic bands of coesite and stishovite have been reported by Boyer et al. (1985), Serghiou et al. (1995), Lounejeva et al. (2002), and Ostroumov et al. (2002). Boyer et al. (1985) found that the strongest coesite line is at 521 cm^{-1}, with other characteristic lines at 117, 177, and 271 cm^{-1}, while Serghiou et al. (1995), in laser-heated diamond cell experiments, found that coesite exhibits 3 relatively strong Raman bands at 489, 552, and 790 cm^{-1}, and stishovite shows a strong peak at 790 cm^{-1}. However, none of these Raman bands were observed in any of our Hospital Hill quartzite samples, in agreement with results of other studies of shocked quartz (e.g., Stöffler and Langenhorst 1994; Grieve et al. 1996).

While the unshocked sample and the 12 GPa samples show Raman spectra with distinct, sharp lines that agree with lines for α-quartz, the spectra of the 25 and 28 GPa samples are characterized by the absence of such sharp lines and by the presence of rather broad bands at lower total intensities (Figs. 4 and 5). We observe that a distinct broad band is centered near 490 cm^{-1} in the spectra of the samples shocked at 25 and 28 GPa, being most pronounced in the spectra of the 28 GPa/25°C sample. McMillan et al. (1992) showed that spectra for pressure-densified SiO_2 glass and diaplectic quartz glass are characterized by bands centered at 490 cm^{-1}, with a second band at about 810 cm^{-1}. This agrees well with the positions of the bands in our spectra of the 25 and 28 GPa samples and indicates the presence of diaplectic SiO_2 glass and/or amorphization associated with the presence of glass-filled PDFs. Champagnon et al. (1996) found from their Raman studies of shocked quartz that the crystalline quartz is converted to the amorphous state between 22 and 32 GPa at room temperature. Our data agree well with this observation, although the dominance of the broad bands in the Raman spectra seems to appear only around 31 GPa in the samples studied by Champagnon et al. (1996). The difference could be a side effect of higher temperatures in our shock experiments, and/or a higher degree of lattice defects in the quartzite used in our experiments.

Cathodoluminescence Spectroscopy

CL-Bright and CL-Dark Areas in Cathodoluminescence (CL) Images

The cathodoluminescence images provide information on the presence of activators and quenchers in the sample. Thus, the CL-bright luminescence of the samples is related to the presence of different inclusions and fractures, as well as defects of the crystal structure and chemical impurities (e.g., Al, Li, and Na; Ramseyer and Mullis 1990; Perny et al. 1992; Demars et al. 1996). However, this also includes slight differences due to the somewhat heterogeneous nature of the natural quartzite. The amorphous state of quartz at high shock pressure and pre-shock temperature is characterized by a lack of recombination centers for photon emissions, which leads to the CL-dark areas and weakly luminescent background of the samples.

CL Spectra of Unshocked and Shocked Samples

The CL spectra of all samples are dominated by broad band/peaks and almost total absence of any sharp emission lines. According to Remond et al. (2000), the peak width of broad CL emission bands indicates that excited and ground states of the electronic radiative transitions are strongly coupled with the vibrating lattice. Stronger coupling indicates that more phonons are emitted after the electronic transition. 1) Broad intrinsic emission generally results from self-trapped excitons (STE), which are highly localized excitons trapped by their own self-induced lattice distortion. STE are generally produced in crystals that are characterized by strong electron-phonon coupling. The emission energy of the STE is usually much lower than the band gap of the material due to the energy lost by phonon emission during the electronic transition; 2) excitation of electrons or holes trapped (dangling bonds in covalent crystals) at point defects, such as vacancies, and interstitial and point defect clusters usually produce broad CL peaks at all temperatures (Remond et al. 2000).

According to Stevens Kalceff et al. (2000, and references therein), the normal defect-free configuration of (low pressure) silicon dioxide polymorphs can be represented as (≡Si-O-Si≡),

indicating that each silicon atom is surrounded by 4 tetrahedrally configured oxygen atoms, and the adjacent silicon atoms are bridge-bonded through a single oxygen atom. The silicon dioxide structure may be modified by the presence of defects (e.g., impurities, vacancies). The dominant observed defects occur in the short-range order involving the slightly distorted SiO_4 tetrahedra, which are common to both the crystalline and amorphous SiO_2 structures. Recently, the detected luminescence bands of the crystalline and amorphous modifications of SiO_2 have been attributed to 3 optically active luminescence centers: 1) two-fold coordinated silicon (=Si:); 2) non-bridging oxygen hole centers; and 3) the STE (Fitting et al. 2001). Fitting et al. (2001) found a red band at 650 nm due to a band-band recombination center, a blue band at 460 nm (triplet-singlet), and an ultraviolet band at 290 nm (singlet-singlet defect luminescence band).

The positions of the broad bands can be interpreted as band-band recombination centers (at around 290 nm in our 12 GPa/100°C sample) and as defect luminescence centers caused by high shock pressure (at around 460 nm in the CL spectra of all 28 GPa samples); these positions are similar to those that have been described for previous CL studies of quartz (Fitting et al. 2001). The broad bands between 330 and 438 nm in our unshocked, 12 GPa (at 100, 450, and 750°C), and 25 GPa (at 750°C) samples might be related to structural imperfections (e.g., Sippel and Spencer 1970). The broad, reddish emission band at 610–650 nm, which was mentioned by Götze et al. (2001) for some shocked quartz, is of low intensity in our samples.

SUMMARY AND CONCLUSIONS

In general, CL images of all samples show CL-bright luminescent patchy areas and bands in otherwise non-luminescent quartz and CL-dark irregular fractures, which could be related to the microdistribution of some activator elements (e.g., Al, Li, Na). The presence of fluid inclusions could be indicated in the CL images of the sample shocked to 25 GPa at 750°C and the sample shocked at 28 GPa and 450°C. Only the optical image of the sample shocked to 28 GPa at 25°C exhibits PDFs, which are, however, neither visible in the BSE nor the CL image, in contrast to observations by Boggs et al. (2001), who noticed a network of bright and dark zones generally corresponding to optical PDFs in shocked quartz from the Ries impact structure.

Cathodoluminescence spectra of unshocked and experimentally shock-deformed samples show broad bands in the near-ultraviolet range and the visible light range at all shock pressures. These broad bands might be associated with defect centers on, e.g., SiO_4^{4-}-groups. Distinct differences exist between the CL spectra of the unshocked and the shocked samples, and shifts in the center positions of the broad bands are evident with increasing shock pressure. This might indicate that recombination centers or traps for the photon emission are more closely-spaced in the band gap between VB and CB as a function of the increasing shock pressure, which is probably caused by partial amorphization.

The Raman spectra with sharp peaks indicate the presence of normal quartz in the unshocked and 12 GPa samples. These peaks disappear in the samples shocked at 25 and 28 GPa, which are dominated by broad bands of about 490 and 820 cm^{-1}. These broad bands indicate a wide range of diffuse vibrational modes and indicate the presence of diaplectic SiO_2 glass.

The results show distinct changes of the CL and Raman properties of quartz with shock pressure and point to a possible use of these methods as shock barometers. Changes based on the pre-shock temperature are less pronounced. A wider range of shock pressures and a variety of quartz and quartzite samples should be studied before any quantification is possible.

Acknowledgments–We thank Ming Zhang (University of Cambridge, UK) for helpful comments, Alan Huffman (Exxon, USA) for providing some of the experimentally shocked samples, and Gero Kurat (Natural History Museum, Vienna, Austria) for access to the SEM-CL facility at the Natural History Museum, Vienna, Austria. We are grateful to L. Nasdala (Mainz) and R. Skala (Prague) for detailed and helpful reviews and to A. Deutsch for editorial comments and support. Laboratory work was supported by the Austrian Science Foundation (grant Y58-GEO, to C. Koeberl). This is University of the Witwatersrand Impact Cratering Research Group Contribution No. 58. A. Gucsik was also supported by a Mobility Grant of the European Science Foundation IMPACT Programme.

Editorial Handling—Dr. Alex Deutsch

REFERENCES

Boggs S., Krinsley D. H., Goles G. G., Seyedolali A., and Dypvik H. 2001. Identification of shocked quartz by scanning cathodoluminescence imaging. *Meteoritics & Planetary Science* 36:783–793.

Boyer H., Smith D., Chopin C., and Lasnier B. 1985. Raman microprobe determination of natural and synthetic coesite. *Physics and Chemistry of Minerals* 12:45–48.

Champagnon B., Panczer G., Chemarin C., and Humbert-Labeaumaz B. 1996. Raman study of quartz amorphization by shock pressure. *Journal of Non-Crystalline Solids* 196:221–226.

Cygan R. T., Boslough M. B., and Kirkpatrick R. J. 1990. NMR spectroscopy of experimentally shocked quartz: Shock wave barometry. Proceedings, 20th Lunar and Planetary Science Conference. pp. 127–136.

Demars C., Pagel M., Deloule E., and Blanc P. 1996. Cathodoluminescence of quartz from sandstones: Interpretation of the UV range by determination of trace element distributions and fluid inclusion P-T-X properties in authigenic quartz. *American Mineralogist* 81:891–901.

Etchepare J., Meriane M., and Smetankine L. 1974. Vibrational modes of SiO_2. I. α and β quartz. *Journal of Chemical Physics* 60:1874–1876.

Faulques E., Fritsch E., and Ostroumov M. 2001. Spectroscopy of natural silica-rich glasses. *Journal of Mineralogical and Petrological Sciences* 96:120–128.

Fitting H J., Barfels T., Trukhin A. N., and Schmidt B. 2001. Cathodoluminescence of crystalline and amorphous SiO_2 and GeO_2. *Journal of Non-Crystalline Solids* 279:51–59.

Fouke B. W., Zerkle A. L., Alvarez W., Pope K. O., Ocampo A. C., Wachtmann R. J., Grajales-Nishimura J. M., Claeys P., and Fischer A. G. 2002. Cathodoluminescence petrography and isotope geochemistry of KT impact ejecta deposited 360 km from the Chicxulub crater, at Albion Island, Belize. *Sedimentology* 49: 117–138.

Götze J., Plötze M., and Habermann D. 2001. Origin, spectral characteristics, and practical applications of the cathodoluminescence (CL) of quartz—A review. *Mineralogy and Petrology* 71:225–250.

Grieve R. A. F., Langenhorst F., and Stöffler D. 1996. Shock metamorphism in nature and experiment: II. Significance in geoscience. *Meteoritics & Planetary Science* 31:6–35.

Halvorson K. and McHone J. F. 1992. Vredefort coesite confirmed with Raman spectroscopy (abstract). 23rd Lunar and Planetary Science Conference. pp. 477–478.

Hayward C. L. 1998. Cathodoluminescence of ore and gangue minerals and its application in the minerals industry: In *Modern approaches to ore and environmental mineralogy,* edited by Cabri L. J. and Vaughan D. J. Mineralogical Association of Canada Short Course Series 27. pp. 269–325.

Huffman A. R., and Reimold W. U. 1996. Experimental constraints on shock-induced microstructures in naturally deformed silicates. *Tectonophysics* 256:165–217.

Huffman A. R., Brown J. M., Carter N. L., and Reimold W. U. 1993. The microstructural response of quartz and feldspar under shock loading at variable temperatures. *Journal of Geophysical Research* 98:22171–22195.

Langenhorst F. and Deutsch A. 1994. Shock experiments on pre-heated α- and β-quartz: I. Optical and density data. *Earth and Planetary Science Letters* 125:407–420.

Langenhorst F., Deutsch A., Hornemann U., and Stöffler D. 1992. Effect of temperature on shock metamorphism of single crystal quartz. *Nature* 356:507–509.

Lounejeva E., Ostroumov M., and Sánches-Rubio G. 2002. Micro-Raman and optical identification of coesite in suevite from Chicxulub. In *Catastrophic events and mass extinctions: Impacts and beyond,* edited by Koeberl C. and MacLeod K. G. Special Paper 356. Boulder: Geological Society of America. pp. 47–54.

McMillan P. F., Wolf G. H., and Lambert P. 1992. A Raman spectroscopic study of shocked single crystalline quartz. *Physics and Chemistry of Minerals* 19:71–79.

Marshall D. J. 1988. *Cathodoluminescence of geological materials.* Boston: Unwin Hyman. 146 p.

Milliken K. L. and Laubach S. E. 2000. Brittle deformation in sandstone diagenesis as revealed by scanning cathodoluminescence imaging with application to characterization of fractured reservoirs. In *Cathodoluminescence in geosciences,* edited by Pagel M., Barbin V., Blanc P., and Ohnenstetter D. Heidelberg: Springer. pp. 225–243.

Okuno M., Reynard B., Shimada Y., Syono Y., and Willaime C. 1999. A Raman spectroscopic study of shock-wave densification of vitreous silica. *Physics and Chemistry of Minerals* 26:304–311.

Ostroumov M., Faulques E., and Lounejeva E. 2002. Raman spectroscopy of natural silica in Chicxulub impactite, Mexico. *Comptes Rendus Geoscience* 334:21–26.

Owen M. R. and Anders H. M. 1988. Evidence from cathodoluminescence from non-volcanic origin of shocked quartz at the Cretaceous/Tertiary boundary. *Nature* 334:145–147.

Perny B., Eberhardt P., Ramseyer K., Mullis J., and Pankrath R. 1992. Microdistribution of Al, Li, and Na in α-quartz: Possible causes and correlation with short-lived cathodoluminescence. *American Mineralogist* 77:534–544.

Poutivcev M., Kempe U., Götze J., Monecke T., Wolf D., and Kremenetsky A. A. 2001. Cathodoluminescence and trace element characteristics of quartz pebbles from the Witwatersrand, South Africa (abstract). In *Cathodoluminescence in geosciences: New insights from CL in combination with other techniques.* Freiberg: Technische Universität Bergakademie. pp. 101–102.

Ramseyer K. and Mullis J. 1990. Factors influencing short-lived blue cathodoluminescence of α-quartz. *American Mineralogist* 75: 791–800.

Ramseyer K. and Mullis J. 2000. Geologic application of cathodoluminescence of silicates. In *Cathodoluminescence in geosciences,* edited by Pagel M., Barbin V., Blanc P., Ohnenstetter D. Heidelberg: Springer. pp. 177–191.

Ramseyer K., Aldahan A. A., Collini B., and Lindström O. 1992. Petrological modifications in granitic rocks from the Siljan impact structure: Evidence from cathodoluminescence. *Tectonophysics* 216:195–204.

Reimold W. U. 1988. Shock experiments with preheated Witwatersrand quartzite and the Vredefort microdeformation controversy (abstract). 19th Lunar and Planetary Science Conference. pp. 970–971.

Reimold W. U. and Hörz F. 1986. Experimental shock metamorphism of Witwatersrand quartzite (abstract). Geocongress '86, Geological Society of South Africa, Johannesburg. pp. 53–57.

Remond G., Phillips M. R., and Roques-Carmes C. 2000. Importance of instrumental and experimental factors on the interpretation of cathodoluminescence data from wide gap materials: In *Cathodoluminescence in geosciences,* edited by Pagel M., Barbin V., Blanc P., and Ohnenstetter D. Heidelberg: Springer. pp. 59–126.

Schmidt C. and Ziemann A. M. 2000. In-situ Raman spectroscopy of quartz: A pressure sensor for hydrothermal diamond-anvil cell experiments at elevated temperatures. *American Mineralogist* 85:1725–1734.

Serebrennikov A. I., Valter A. A., Mashkovtsev R. I., and Scherbakova M. Y. 1982. The investigation of defects in shock-metamorphosed quartz. *Physics and Chemistry of Minerals* 8: 153–157.

Serghiou G., Zerr A., Chudinovskikh L., and Boehler R. 1995. The coesite-stishovite transition in a laser-heated diamond cell. *Geophysical Research Letters* 22:441–444.

Seifert, F., Mysen B. O., and Virgo D. 1982. Three-dimensional network structure of quenched melts (glass) in the systems SiO_2-$NaAlO_2$, SiO_2-$CaAl_2O_4$, and SiO_2-$MgAl_2O_4$. *American Mineralogist* 67:696–717.

Seyedolali A., Krinsley D. H., Boggs S., O'Hara P. F., Dypvik H., and Goles G. 1997. Provenance interpretation of quartz by scanning electron microscope-cathodoluminescence fabric analysis. *Geology* 25:787–790.

Sippel F. R. and Spencer B. A. 1970. Luminescence petrography and properties of lunar crystalline rocks and breccias: In *Proceedings of the Apollo 11 Lunar Science Conference,* edited by Levinson A. A. New York: Pergamon Press. pp. 2413–2426.

Stevens Kalceff M. A., Phillips M. R., Moon A. R., and Kalceff W. 2000. Cathodoluminescence microcharacterisation of silicon dioxide polymorphs: In *Cathodoluminescence in geosciences,* edited by Pagel M., Barbin V., Blanc P., and Ohnenstetter D. Heidelberg: Springer. pp. 193–224.

Stöffler D. and Langenhorst F. 1994. Shock metamorphism of quartz in nature and experiment: I. Basic observations and theory. *Meteoritics* 29:155–181.